2001-01-0529

The Influence of Injector Parameters on the Formation and Break-Up of a Diesel Spray

R. Morgan and J.Wray
Ricardo

D.A.Kennaird, C.Crua and M.R. Heikal
University of Brighton

ABSTRACT

The influences of injector nozzle geometry, injection pressure and ambient air conditions on a diesel fuel spray were examined using back-lighting techniques. Both stills and high speed imaging techniques were used. Operating conditions representative of a modern turbocharged aftercooled HSDI diesel engine were achieved in an optical rapid compression machine fitted with a common rail fuel injector.

Qualitative differences in spray structure were observed between tests performed with short and long injection periods. Changes in the flow structure within the nozzle could be the source of this effect.

The temporal liquid penetration lengths were derived from the high-speed images. Comparisons were made between different nozzle geometries and different injection pressures. Differences were observed between VCO (Valve Covers Orifice) and mini-sac nozzles, with the mini-sac nozzles showing a higher rate of penetration under the same conditions.

INTRODUCTION

Developments in engine simulation technology have made the 'virtual engine' model a realistic proposition [1]. The use of Computational Fluid Dynamics (CFD) on engine development programs has enabled significant time and cost savings to be made in the design and development of the engine combustion system. Accurate modelling of the fuel spray formation and mixing process is a key part of a successful combustion simulation.

Several spray break up models have been proposed in recent years [2,3,4] and have yielded good results when implemented in commercial CFD codes [5]. Accurate simulation of the fuel spray formation process can be achieved by inputting measured data as a boundary condition into the simulation, such as spray cone angle and droplet distribution from calibration tests on the fuel system in question. However, a preferable approach is to be able to simulate the influence of the injector design on spray formation by inputting readily available geometric parameters alone into an empirical model or direct simulation of the internal flow within the injector. Either approach requires extensive validation to ensure the correct boundary conditions are derived across the expected operating range of the engine.

In order to check the validity of the fuel spray model, an extensive experimental program has been undertaken by Ricardo to gather data on the spray formation and break-up process at conditions representative of modern and future diesel engines. A rig has been installed at the University of Brighton to enable research on the fuel spray to be performed using a modern common rail fuel system at conditions representative of those found in a diesel engine. The first phase of this work, reported in this paper, covers imaging work on the fuel spray over a wide range of test conditions. The influence of injection pressure and nozzle geometry on the behaviour of the fuel spray has been studied at a range of ambient pressure and temperature conditions. The results, in terms of the liquid penetration length and dispersion angle have been compared with a number of established empirical models.

BACKGROUND

The modern turbocharged aftercooled (TCA) diesel offers an efficient, low emissions automotive power plant. The fuel system has and will continue to play a vital role in the development of improved diesel engines for the foreseeable future [6]. The data presented in Figure 1(a) shows how fuel injection pressure has risen over the last 30 years. Research has shown that there are still benefits to be realised by

further increasing the injection pressure and rate [7], but these developments may proceed at a slower rate due to the technical challenges of further increasing the injection pressure within the constraints of low cost and high reliability. Parallel developments in the design of the injector nozzle have led to a reduction in sac volume with the introduction of mini-sac and VCO (valve covers orifice) nozzles and a consequent improvement in engine hydrocarbon emissions [8].

Although the advantages of increasing fuel pressure have been outlined, a modern HSDI engine still requires fuel injection equipment to deliver at lower rail pressures and fuelling quantities during the lower load and speed operating points. A typical fuelling map is shown in Figure 1 (b). Since emission legislation drive cycles require operation within these regimes, research into these lower fuel pressure areas is of great importance.

Both injection pressure [9] and nozzle design [10,11] have been shown to influence the behaviour of the fuel spray during the formation and break-up process prior to auto-ignition. Two processes must be considered. First, the macro effect on the spray from the introduction of fuel to the combustion chamber at higher velocities through a small orifice. This has a strong influence on the entrainment of air and subsequent break-up of the fuel spray [9]. Second, the fuel pressure and nozzle design will also affect the flow behaviour of fuel inside the nozzle, possibly introducing separation and cavitation within the nozzle [12,13]. In extreme cases this can result in hydraulic flip and a dramatic change in the structure of the spray [14]. Therefore the internal flow inside the nozzle must also be considered as well as the direct 'entrainment' process when modelling the external spray formation and break up processes.

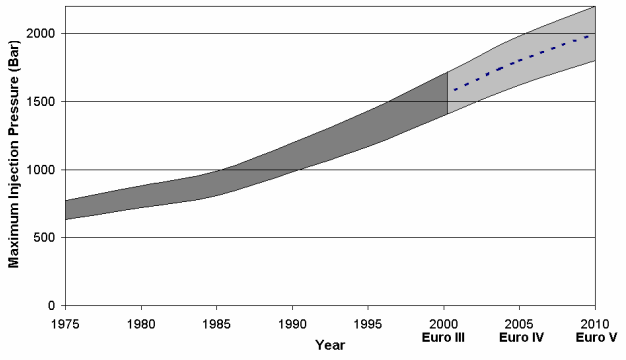

Figure 1 (a) Past and projected trends in fuel injection pressure

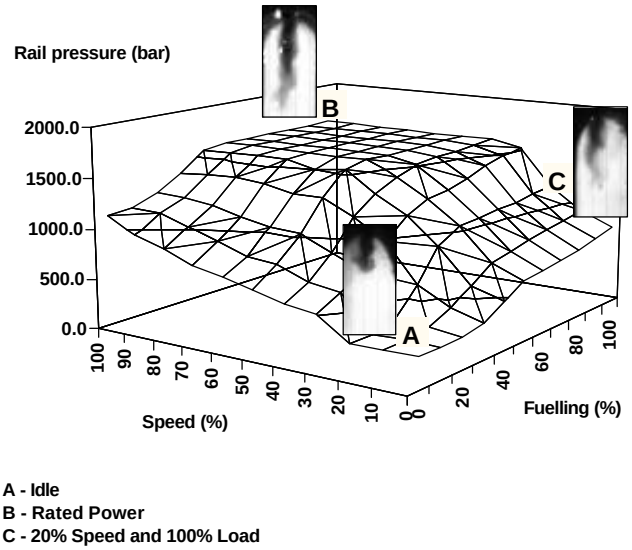

A - Idle
B - Rated Power
C - 20% Speed and 100% Load

Figure 1 (b) Typical HSDI fuelling map

INFLUENCE OF FUEL PRESSURE - Several researches have attempted to simulate the effect of fuel pressure P_f, or more commonly the pressure difference across the nozzle, DP on spray tip penetration, S and dispersion angle, q. The theoretical dependence of nozzle pressure difference was derived by Naber and Siebers [9] and reported as:

$$S \propto (\Delta P)^{0.25}, \text{ where } \Delta P = P_f - P_a.$$

Similar dependence was found by Hiroyasu and Arai [15] and Dent [16]. Arregle *et al.* [17] produced an empirical model with the following dependence on fuel pressure:

$$S \propto P_f^{0.262}$$

There is therefore good agreement in the literature on the influence of nozzle pressure difference on spray penetration. Figure 2 shows the comparative effects of changing injection pressure on spray penetration for the models discussed. As expected, the rate of penetration is predicted to be similar in the four models considered but the absolute penetration is observed to differ by up to 5 mm at 1 ms after the start of injection. This equates to a potential error of 10% in spray tip position for an automotive sized engine at moderate engine speed and could result in a significant mismatch of the combustion system to the injection system resulting in poor performance of the engine.

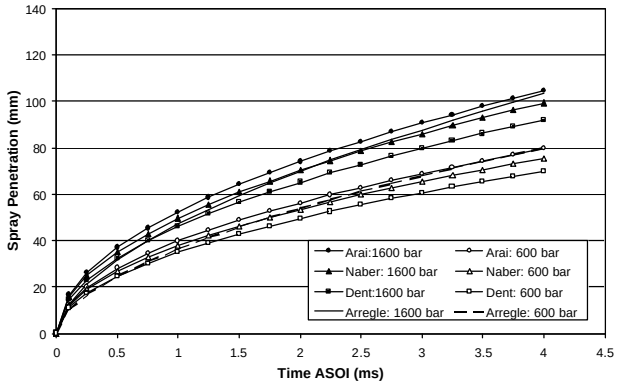

Figure 2 Comparison of predicted penetration rate for various models

The empirical model to predict spray angle proposed by Naber and Siebers [9] has no direct dependence on fuel pressure, however it is sensitive to fuel density. Arregle *et al.* [17] found that there was no spray angle dependence on fuel injection pressure as the fitted exponent varied between –0.00967 and 0.0284.

The effect of the internal flow within the nozzle has been studied by a number of research groups [12,13,14]. Cavitation has been shown to affect the flow in the nozzle orifice and consequently the spray structure particularly in a VCO nozzle [14]. Nozzle hole diameter and nozzle length is included in some of the established correlation's [9,15,16,17] but it is unclear as to whether these parameters alone are sufficient to predict the behaviour of the fuel spray from knowledge of the nozzle designs. The critical parameter is likely to be the cavitation number, defined as:

$$Ca = \frac{\Delta P}{P_v}$$

Where P_v is the vapor pressure of the fuel. However, geometric factors such as the entry radius of the orifice [18] are also known to influence the onset of cavitation. Research has shown a number of stages in the development of nozzle cavitation and the subsequent effect on the fuel spray structure [14]. The transition is not observed to be smooth so a simple relationship is unlikely to predict the observed result. Further work is required to understand and subsequently model the effect of nozzle flow on the fuel spray formation process.

The discrepancy in penetration shown in Figure 2 could be due to differences in the characteristics of the injectors used by the four research groups. Fuel systems have different nozzle geometry and injection rate profiles which would result in different fuel velocities at the nozzle exit and different absolute differences in penetration but similar penetration rates.

INFLUENCE OF AIR DENSITY - Air density has been identified as a critical variable in most of the more widely used correlations [9,15,16,17]. The air will have a drag effect on the fuel spray resulting in dissipation of the spray energy and a consequential slowing down of the fuel. The interaction of the fuel and air also results in entrainment of air with the evolving fuel spray which is thought to be an important mechanism driving the break-up of the diesel fuel spray [19].

The models proposed by Dent [15] and Hiroyasu and Arai [16] have the same dependence on air density and in-cylinder pressure:

$$S \propto \left(\frac{P_f - P_a}{\rho_a} \right)^{0.25}$$

Using the Naber and Siebers [9] model and including the empirical model developed to predict spray dispersion angle, the following dependence is shown:

$$S \propto \frac{\left(P_f - P_a\right)^{0.25}}{\left(r_a\right)^{0.345}}$$

The Arregle *et al.* [17] model shows a far higher penetration dependence on air density than the other models:

$$S \propto \left(r_a\right)^{-0.406}$$

The effects of these differences are shown in Figure 3. This result suggests there is less agreement in the literature on the influence of air density. The empirical model developed by Naber and Siebers [9] for cone angle is dependent on air density as shown:

$$Tan\left(\frac{q}{2}\right) \propto \left(r_a\right)^{0.19}$$

Whereas Arregle *et al.* [17] found the density exponent was higher at around 0.335.

In summary, a number of different correlations for both spray tip penetration and dispersion are reported in the literature. There is broad agreement in the trends predicted by these correlation's but the quantitative correlation is poor between different models. The influence of injector nozzle design has not been considered in detail and may be the reason for some of the disagreement between different studies. Future engine designs are likely to operate at increased injection pressures than those typically found today so continued work is required to test the validity of the spray models at ever higher fuel injection pressures.

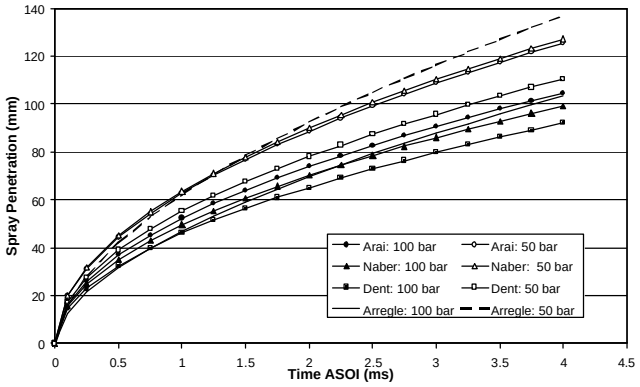

Figure 3 Comparison of predicted penetration rate for varying air density

EXPERIMENTAL APPARATUS

HIGH PRESSURE SPRAY RIG - A high pressure and temperature spray and combustion research facility was installed in 1999 at The University of Brighton in the United Kingdom. The facility was designed to enable spray and combustion studies to be performed at conditions representative of a modern TCA diesel engine. The design of the new facility has been described in the past [20,21]. The main features are:

- Independent control of air pressure and density
- Air pressures in the range of 3 to 13 MPa
- Air temperatures in the range of 570 K to 1000 K
- Multiple consecutive injections of fuel
- Quiescent air motion during the injection and spray formation process

The rig is based on a rapid compression machine with a large optical chamber into which the spray is introduced. The chamber is 50 mm in diameter and 70 mm long. Interaction with the wall would be expected to be minimal for a fuel spray of the type produced by an injector used in a passenger car engine. A schematic of the spray chamber is shown in Figure 4.

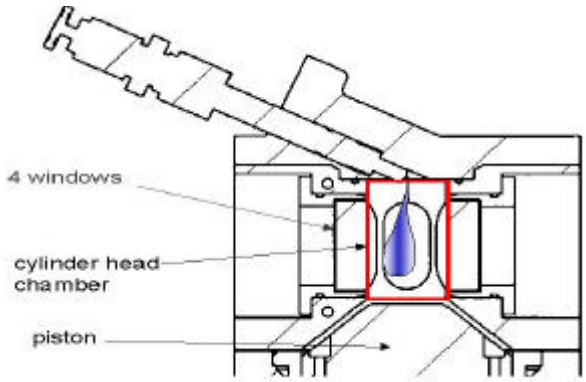

Figure 4 Schematic of the spray chamber

The air pressure and temperature at the start of injection are controlled by conditioning the charge air into the engine by means of an air compressor and heater. The inducted air is then compressed in the engine to the desired test conditions. CFD analysis has previously confirmed the air motion is essentially quiescent [21]. The maximum air velocity in the chamber during the injection process was predicted to be less than 1 m/s in the axial direction of the spray.

FUEL SYSTEM - A second generation Bosch common rail system [22] was used for this work, with a maximum rail pressure capability of 160 MPa. The fuel pump was powered by an electric motor running at 1400 rev/min which ensured a stable rail pressure with minimal fluctuation. The rail and delivery pipe were both instrumented with a 4067 Kistler pressure transducer. The pipe from the rail to the injector was kept short, representative of a passenger car. A custom controller [21] was manufactured to enable independent control of injection timing, injection duration and rail pressure. A number of nozzles were used in this study, as summarised in Table 1.

Nozzle Type	Orifice diameter (mm)	Lift / diameter (L/d)
VCO	0.10	10.0
VCO	0.15	6.8
VCO	0.20	5.0
Mini-sac	0.10	10.0
Mini-sac	0.15	6.8
Mini-sac	0.20	5.0

Table 1: Details of nozzles used in the study

The nozzles were of a single-hole design with an equivalent cone angle of 130°. The holes were manufactured by a conventional spark erosion technique and then micro-honed to produce an entry radius and surface finish representative of a production nozzle. The needle was of the double guided type and was instrumented with a Hall effect type needle lift sensor. Previous work [14] has shown hole to hole variability due to poor concentricity of the needle within the VCO nozzle. Ambient pressure spray imaging, shown in Figure 5, of a single hole nozzle was performed to confirm the general spray structure was representative of the multi hole nozzle. The results suggest the single hole nozzle produces a representative spray structure in this case.

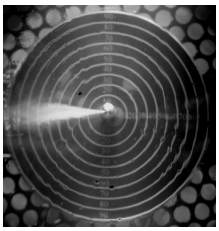

Figure 5 Spray from a single hole nozzle under

ambient conditions

INJECTOR CALIBRATION - The complete fuel system, including pump, rail, pipe-work and controller was calibrated on a Lucas rate gauge. This was initially done to verify that the new controller matched the injection rate diagram produced from a Bosch production Engine Control Unit (ECU). The injection rate diagrams shown in Figure 6 show that an equivalent injection rate diagram to that of a typical common rail fuel system was achieved using the custom controller. Each of the nozzles was calibrated to establish a correlation between injection duration and injected fuel mass. Fuel flow was not measured during the imaging experiments but was derived from the injection duration and nozzle calibration. The same injector was used for the duration of these experiments. The injection rate was checked on the Lucas rate gauge after each nozzle change to confirm that the injector was performing correctly prior to testing on the spray rig.

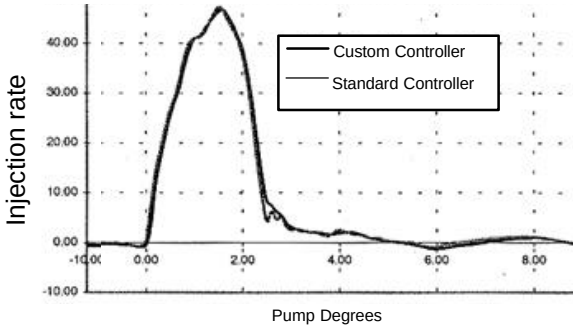

Figure 6 Injection rate diagram from standard and custom controller

EXPERIMENTAL TECHNIQUE

GENERAL TEST PROCEDURE - The spray rig was set up prior to each test by pre-heating the cylinder head and liner to 80 °C. In addition, the inlet pipe-work was pre-heated for the hot tests by flushing through with heated air. The air temperature and pressure at TDC were controlled by pre-conditioning the charge air to the desired temperature and pressure and compressing to the test conditions. The back pressure across the engine was set to maintain good scavenge efficiency and acceptable air flow. The cylinder pressure, fuel pressure and needle lift were captured on a digital storage scope and system temperatures and pressures on a low speed data logger. The low-sulphur diesel used for all the tests had the following properties:

- Density 840 kg/m^3
- Cetane Number 51
- Sulphur Content < 0.03%

In the work presented a number of injection strategies were considered covering representative fuelling quantities from pilot through to heavy load conditions, as shown in Table 2. The total amount of fuel injected was calculated from the injection duration.

Injection pressure (MPa)	Orifice diameter (mm)		
	0.2	0.15	0.1
60	Fuelling quantities from 3 - 50 mm^3		
100			
140			
160			

Table 2: Fuel injection conditions studied

STILLS PHOTOGRAPHY - A fully manual Pentax still camera was used with a telephoto lens (125 mm, f:1/4-1/22) and two extension tubes (1+3 cm). This combination was found to give the best compromise between magnification and focal distance. During the tests, a high-speed argon flash lamp was synchronized with the engine and delayed relative to TDC by means of the fuel system controller. For each photograph, the shutter of the camera was kept open until an injection occurred. A diffused back-lighting was preferred to side-lighting for a more homogeneous illumination of the spray background. The duration of the flash was about 3µs. The backlit images provide an area-integrated image of the fuel spray.

Kodak 400 ISO films were used and the camera aperture was set to f:1/8. These settings were found to give a good compromise between sensitivity of the film, quality of the prints and depth of field (measured to be about 4 mm at f:1/8). Even though a smaller lens aperture would have provided a much larger depth of field (i.e. better focusing of the whole spray), the amount of light available with the argon flash-gun was not sufficient to give correct exposure.

For each one of the three different fuelling rates tested, two photographs were taken at different timings: one around the maximum liquid length and one showing the break up of the spray. Because the tip of the nozzle was not visually accessible through the windows, the beginning of the injection could not be observed. Excellent repeatability was obtained, in terms of both liquid penetration length and spray cone angle.

As the tests were done under backlighting, the shape of the back window can clearly be seen on each photograph. After correcting for optical distortion, the

actual dimensions of the optical window were used to derive a scaling factor for the photographs.

HIGH SPEED IMAGING - The CCD video camera used in this series of experiments was a Kodak Ektapro HS Motion Analyzer (Model 4540), with a recording rate adjustable from 30 to 4500 frames per second at full resolution (256×256 pixels × 256 grey levels), and from 9000 to 40500 frames per second at progressively reduced resolution. The best compromise between acquisition rate and image resolution was obtained with a frame rate of 18000 pictures per second, with a corresponding resolution of 256×64 pixels × 256 levels of grey. The camera was used in the intensified gain mode, with a gamma correction factor of 1.0 in order to maximize the intensity of the recorded images. The camera was triggered off the injection pulse.

IMAGE PROCESSING - A typical unprocessed image is shown in Figure 7a, the spray nozzle tip is located 20 mm to the right of the window edge and is therefore not visible. The spatial resolution was calculated to be 0.36 mm per pixel.

The images were thresholded to pick out the spray outline from the background. The threshold level was manually chosen by selecting one image from the batch of images generated by a test run and varying the threshold to obtain optimum results. Since the quality of the images was constant during a test run, this threshold value was suitable for all the images in that batch.

The analysis software calculated the spray penetration and spray dispersion angle for each image, the results of which were saved as an Excel spreadsheet, or in graphical format as seen in Figure 7b.

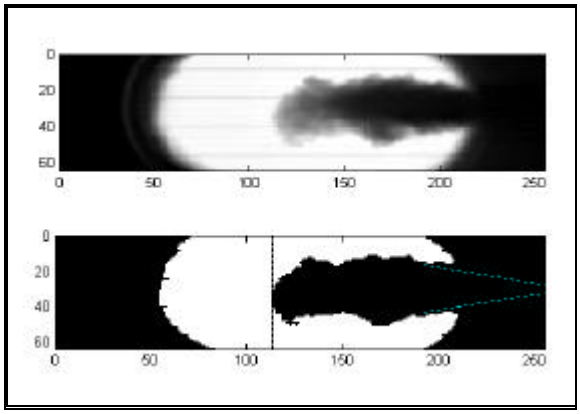

Figure 7 (a) Raw digital spray image (b) Thresholded image showing maximum penetration length

The spray penetration was measured in two ways; firstly the maximum spray penetration was calculated by finding the spray pixel furthest from the nozzle. This value of penetration was then used to calculate the spray angle at half the maximum penetration length.

Once the spray angle was known the spray penetration was calculated using a second method, described by Naber and Siebers [9]; this defines spray penetration as "the distance along the spray axis to a location where ½ of the pixels on an arc of θ/2 centred on the spray axis are dark", this definition was simplified for computational reasons and a straight line was used instead of an arc as shown in Figure 8. This modification was found to make little difference to the values of penetration calculated compared with the method described by Naber and Siebers [9].

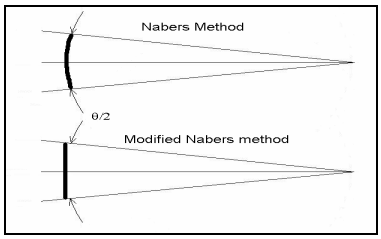

Figure 8 Definition of spray penetration length

By using the value of maximum penetration to calculate the spray angle the iterative approach used by Naber and Siebers [9] was avoided. In most cases there was very little difference between the maximum penetration and the penetration calculated using the modified Naber and Siebers [9] criteria.

ACCURACY OF MEASUREMENT - The calculated results were found to be insensitive to the threshold level chosen with a 12.5% variation in threshold level giving a 1% change in measured penetration. The spray angles calculated have a larger margin of error due to the nozzle tip not being visible in the image. The location of the nozzle tip relative to the window edge was accurately measured but some error can be introduced due to camera shake.

RESULTS AND DISCUSSION

Preliminary laser sheet imaging [20] identified a number of areas of interest for high-resolution photography. Photographic tests were performed at:

- Fuel pressures between 60 and 160 MPa
- Ambient air pressures between 3 and 8MPa
- Ambient air temperature of 540K
- Injection duration from 0.9 to 3.41 ms
- Single-hole VCO nozzle with 0.2mm diameter

A sequence of images taken 1ms after the start of injection for a 3.41ms injection is shown in Figure 9. The images were taken at two values of ambient pressure and four values of rail pressure at an ambient

temperature of 540K. The spray can be considered essentially non-evaporating at this temperature. The expected increase in penetration resulting from an increase in injection pressure or decrease in air pressure is observed. The structure of the spray is consistent with previous observations [23, 24], with areas of atomised droplets being entrained at the edge of the spray where fuel air interaction takes place. The influence of air density can be clearly seen between Figures 9a and 9b, with the higher air density resulting in a noticeable reduction in spray tip penetration, particularly for the lower injection pressures.

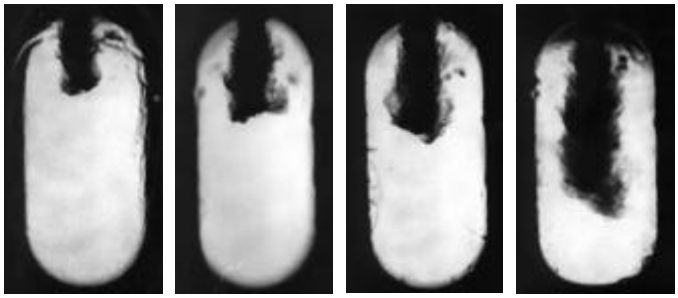

60 MPa 100 MPa 130 MPa 160 MPa

Figure 9 (a) Back lit spray images taken 1 ms after the start of injection in air at 3 MPa with an injection duration of 3.41 ms at four fuel rail pressures

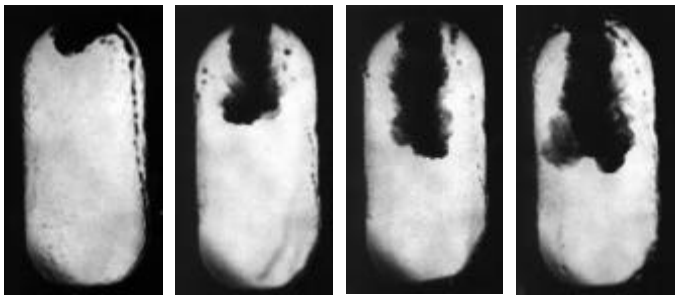

60 MPa 100 MPa 130 MPa 160 MPa

Figure 9 (b) Back lit spray images taken 1 ms after the start of injection in air at 8 MPa with an injection duration of 3.41 ms at four fuel rail pressures

During initial stages of injection a concentrated "bunching" of spray at the leading edge of the jet is formed as droplets penetrate the stagnant gas field, re-circulating areas of droplets are observed to "peel" back along the edge of the spray cone from this area. This droplet stripping process was observed for all injection conditions and is depicted in the sequence in Figure 10 (negative images have been used to increase clarity). The formation of a head vortex due to the entrainment of dense air can be seen more clearly at the higher air density cases.

A similar sequence of images is shown in Figure 11a and 11b for a 0.9 ms injection duration. The spray structure is observed to be slightly different when compared with the 3.41 ms injection case. In the 0.9ms period case, the injector needle will only briefly achieve full lift, resulting in a throttling of the fuel flow under these conditions. Fuel is therefore predominantly injected during throttling, hence the orifice internal flow structure would be expected to be different to that of the 3.41 ms case. This effect has been observed in steady state large scale nozzle tests [14] particularly with VCO nozzles. It demonstrates the importance of understanding the effect of internal orifice flow structure on the behavior of the spray.

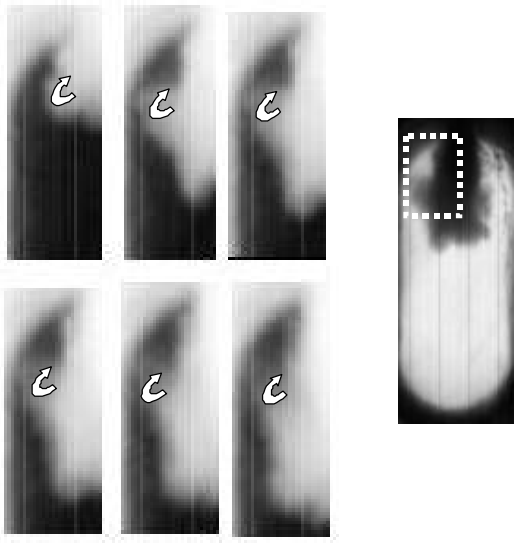

Figure 10 Development of areas of droplets "peeling" back along the spray plume. Enlarged images presented are from 1.1ms ASOI to 1.4 ms ASOI.

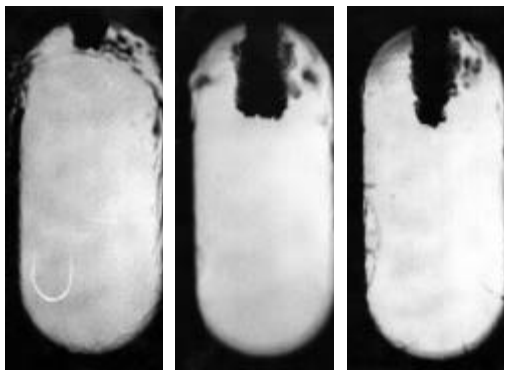

60 MPa 100 MPa 130 MPa

Figure 11 (a) Back lit spray images taken 0.9 ms after the start of injection in air at 3 MPa with an injection duration of 0.9 ms at three fuel rail pressures

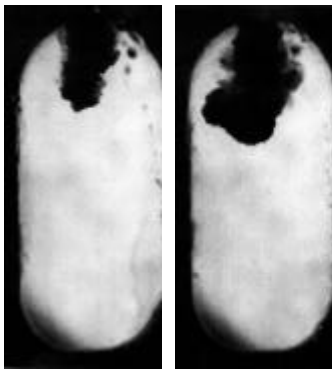

100 MPa 130 MPa

Figure 11 (b) Back lit spray images taken 0.9 ms after the start of injection in air at 8 MPa with an injection duration of 0.9 ms at two fuel rail pressures

INFLUENCE OF FUEL PRESSURE - Figure 12 shows the effects of increasing fuel rail pressure on a VCO (0.2mm) nozzle spray.

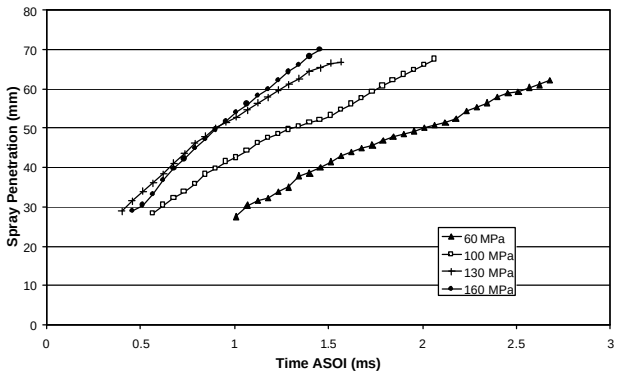

Figure 12 Comparison of experimental penetration rate for varying fuel rail pressures (0.2 mm VCO)

As expected, higher rail pressures result in a higher rate of spray tip penetration. It was however found that there was little difference between 160 and 130 MPa rail pressure results. Spray penetration is generally reported to be a function of the pressure difference across the nozzle:

$$S \propto (\Delta P)^{0.25}$$

According to this relationship, the effect on penetration of a change in injection pressure would be reduced at higher injection pressures. Similarly injector body and nozzle throttling and hence pressure loss becomes more significant for increasing fuel rail pressures. These features could explain the observed result. In addition, it has been previously reported that higher injection pressures result in an increase in the atomisation rate of the spray and result in a decrease in the mean liquid droplet size [25]. It would be expected that the smaller droplets would evaporate at a higher rate, possibly resulting in a reduction in the apparent liquid length of the spray. The imaging technique used in this work will only detect liquid fuel and so evaporation could also influence the ultimate liquid penetration length. Schlieren photography will be used to test this hypothesis in the near future.

INFLUENCE OF NOZZLE TYPE - Two nozzle designs and three nozzle geometries were tested. The main dimensions are summarised in Table 1. Figure 13 shows a comparison of penetration rate at one operating condition (in-cylinder pressure =12MPa; rail pressure = 100MPa). The fuelling amount per injection was maintained constant by changing the injection period.

A higher penetration rate is observed for the larger nozzle orifice diameters and for the mini-sac compared to VCO nozzle. The smaller diameter orifice would be expected to produce a finer more atomised spray. Again, the higher evaporation rate of the smaller droplets could explain the observed result. The difference between the two nozzle designs is interesting. None of the empirical models considered account for geometry upstream of the orifice which is the only difference between the two configurations. Previous work by Heimgärtner and Leipertz [26] has reported the mean droplet size from a VCO nozzle can be up to 50% smaller than the equivalent mini-sac nozzle. Again, this would result in a higher rate of evaporation and could explain the observed result. It has also been shown that VCO nozzle injectors cause a greater pressure loss within the nozzle geometry hence a lower 'Δp' at the nozzle orifice and lower spray penetration. These results emphasises the importance of understanding the influence of nozzle and injector geometry on fuel sprays.

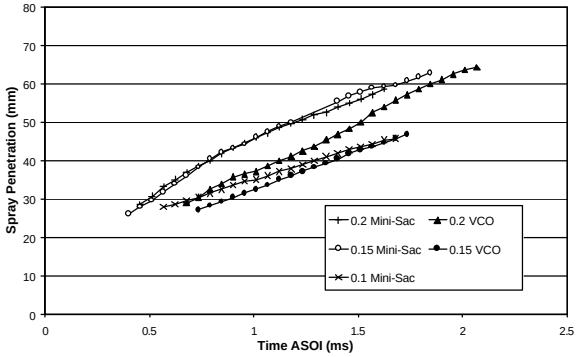

Figure 13 Comparison of experimental penetration rate for varying nozzle sizes and types

INFLUENCE OF AIR TEMPERATURE - Tests were carried out under two temperature conditions. The intake air was heated such that the in-cylinder temperature at "top dead centre" (TDC) was 577K or 701K. Evaporation will occur at both test conditions, but at a much slower rate at 577K. The increase in air temperature between the two conditions will also result

in a decrease in air density of around 14 kg/m^3. The models considered predict that a rise in temperature will cause the spray penetration rate to increase due to the lower air density as shown by the Naber and Siebers [9] model, Figure 14.

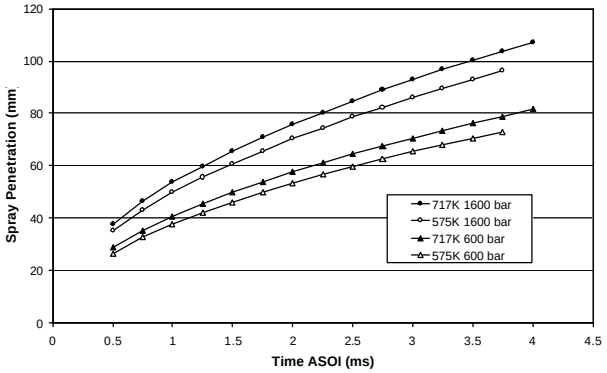

Figure 14 Naber and Siebers [9] model predictions showing the effect of in-cylinder temperature on spray penetration for two different pressures (0.2 mm VCO)

The range of data used to investigate the model presented by Naber and Siebers [9] was gathered over a wide range of ambient air densities, temperatures, injection pressures and nozzle diameters. The range of injection pressures and ambient air densities for the present work and that used in the experiments of Naber and Siebers [9] are presented in Figure 15. The injection nozzle parameters and ambient temperature conditions are presented in Table 3. The injection profile used in the work of Naber and Siebers [9] used a non-rate shaped top hat profile unlike that presented in the current work. The differences above should be appreciated when comparing the data sets from both experiments, especially when considering low fuelling when the injector needle will only partially achieve full lift.

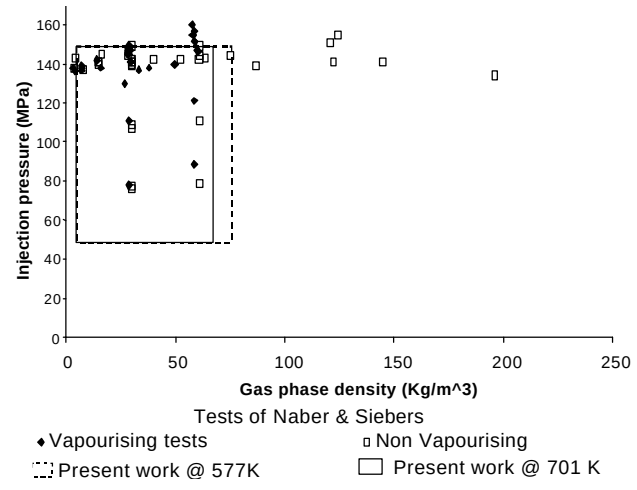

Figure 15 Comparison of range of injection conditions for the present work and that of Naber and Siebers [9] used to develop their penetration model.

	Naber and Siebers	Present work
Nozzle type	Mini-sac	VCO and Mini-sac
Orifice diameter (mm)	0.198 - 0.340	0.1 - 0.2
Orifice off-axis angle (°)	34	65
Gas phase temperature (K)	300 - 452, non-evaporating spray	507
	607 - 1405, evaporating spray	701

Table 3 Injection conditions and nozzle types used

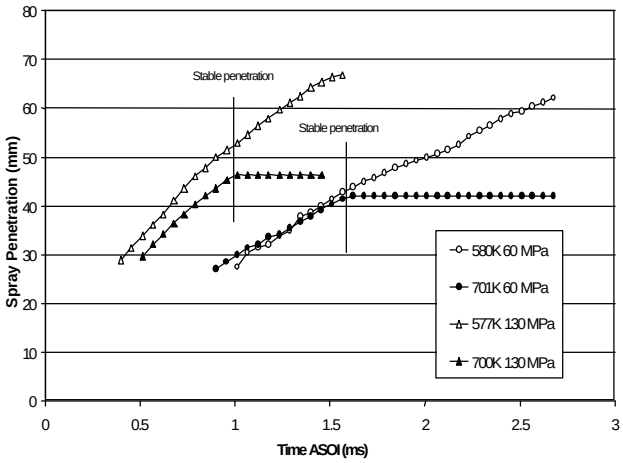

Figure 16 Experimental data showing the effect of in-cylinder temperature on spray penetration for two injection pressures, 60 and 130 MPa

According to Naber and Siebers [9] the effect of ambient temperature changes (600-1400K) on the spray penetration was negligible in conditions of high density, representative of the conditions presented in this work (density > 28.6 kg/m^3). As shown in Figure 16, the penetration rate was found to be similar at 60 MPa rail pressure for the two test temperatures, supporting Naber and Siebers' conclusion. The stable penetration length is observed to be significantly shorter for the higher temperature case as would be expected due to the higher evaporation rate.

The experimental results (Figure 16) do not however support the observation of Naber and Siebers [9] in the

case of higher injection pressure. The higher injection pressure case shows a reduction in penetration rate with increasing temperature, again despite the reduction in air density. For the higher injection pressure, the rate at which fuel enters the chamber is higher[1], increasing the spray cooling effect and creating a local rise in ambient density around the penetrating spray. Subsequent injected fuel has to penetrate this denser environment, leading to a reduction in spray penetration.

In both high temperature cases the ultimate spray length is observed to be similar i.e. independent of injection pressure. The stable core length at 130 MPa is however achieved more rapidly than in the 60 MPa case. All sprays injected into higher temperature environments were observed to reach a stable penetration length and maintain this level of the penetration until the end of the injection period. Similar effects have been observed by others investigating evaporating sprays [27].

Of the current models considered [9,15,16,17], only Dent [15] includes a term to compensate for evaporation:

$$S \propto \left(\frac{294}{T_a} \right)^{0.25}$$

This term however does not compensate enough to predict the results shown in Figure 16. The model predicts a 5% change in penetration whereas a 13-18% change is observed. Although some of the difference may be attributed to different initial injection conditions (nozzle type, off axis angle etc.), further work is required if the influence of evaporation is to be effectively modelled in a simple empirical relationship.

In Figure 17 a direct comparison of experimental penetration measurements are presented with predictions from the model presented by Naber and Siebers [9]. Under these conditions the model over-predicts penetration when compared to both the low and high temperature experimental cases, although there is some agreement for the penetration of the low temperature case in the later stages of injection. These differences again may be attributed to differences in nozzle geometries and injection rate shapes between this work and the experiments used in deriving the relationships. Caution should be applied when predicting penetration from such relationships, it is evident that the temperature effect of reducing liquid penetration to a stable constant length is not predicted by any of the reviewed models, subsequently application of these models may lead to substantial over prediction of spray penetration.

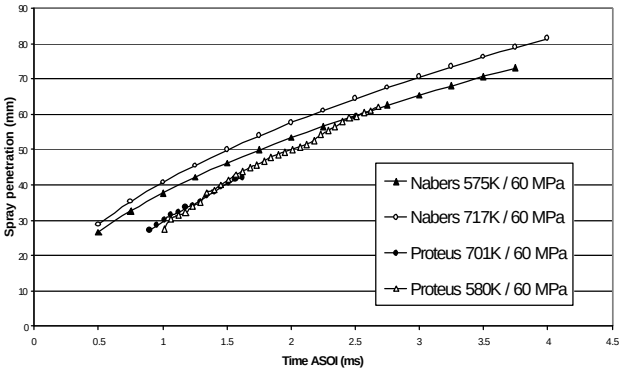

Figure 17 Comparison of experimental and predicted penetration

[1] The injection period is reduced to maintain the fuelling amount constant

CONCLUSIONS

The influences of nozzle tip geometry, ambient pressure and temperature and fuel pressure were studied over a range of conditions representative of a modern diesel engine. Significant differences in spray structure were observed between long and short injection periods. This could be due to differences in internal flow structure within the nozzle at low needle lift.

The expected trends with injection pressure were observed, except at high injection pressure where a lower rate of penetration than expected was observed. The effect on penetration of a change in injection pressure is reduced at higher injection pressures. In addition, the increased rate of evaporation at high injection pressures may also influence the penetration rate of the spray.

The VCO nozzles were observed to show a lower rate of penetration than mini-sac nozzles of the same dimensions. It is proposed that this is due to better atomisation of the spray from the VCO nozzle, possibly due to differences in internal flow structure, resulting in a higher rate of evaporation.

Temperature was observed to affect the rate of liquid penetration when keeping ambient pressure constant. The effect was most pronounced at high injection pressures where the mean droplet size would be expected to be small. The rate of injection was also shown to have an effect on the local cooling of the gas adjacent to the penetrating spray, causing a retardation of the vaporising sprays at higher fuelling rates. This effect, coupled with faster evaporation of the smaller droplets which are produced at higher injection pressures, is suggested as the cause of the apparent reduction in spray tip penetrations. Further investigation is planned in this area.

Caution should be exercised when applying models to predict spray penetration and particular attention should be focused on the injection conditions and nozzle geometry. In the current work, it was found that the effect of injecting into high temperature conditions was to shorten penetration and that penetration length stabilised after a certain injection duration. This effect was not captured in the existing penetration models studied.

ACKNOWLEDGMENTS

The authors would like to thank Mr Wood and Mr Whitney of The University of Brighton and Mr West at Ricardo for their assistance in gathering the data used in this paper. Thanks must also go to the EPSRC, UK for the loan of the high-speed camera equipment. We would also like to thank the directors of Ricardo for allowing the publication of this paper.

REFERENCES

1. G. Li, S.M. Sapsford and R.E. Morgan. CFD Simulation of a DI Truck Diesel Engine Using Vectis. SAE2000-01-2940
2. M.A. Patterson and R.D. Reitz. Modeling the Effect of Fuel Spray Characteristics on Diesel Engine Combustion and Emissions. SAE980131
3. R.D. Reitz and R. Diwakar. Effect of Drop Breakup on Fuel Sprays. SAE860469
4. A.B. Liu, D. Mather and R.D. Reitz. Modeling the Effects of Drop Drag and Breakup on Fuel Sprays. SAE980073
5. C. von Kuensberg Sarre, S.-C. Kong and R.D. Reitz. Modelling the Effects of Injector Nozzle Geometry on Diesel Sprays. SAE1999-01-0912
6. P.L. Herzog. Fuel Injection –The Key to Effective Low-Emission Diesel Engines. IMechE S492/K1/99
7. N.S. Jackson. The High Speed Direct Injection Diesel Engine - Future Potential. THIESEL 2000, Valencia 13-15 September 2000.
8. A. Ilyama, Y. Matsumoto, K. Kawamoto, T. Ohishi. Spray Formation Improvement of VCO Nozzle for DI Diesel Smoke Reduction. IMechE Conference on Diesel Fuel Injection Systems 1992.
9. J. Naber and D.L. Siebers. Effects of Gas Density and Vaporization on Penetration and Dispersion of Diesel Sprays. SAE960034
10. D. Potz, W. Christ and B. Dittus. Diesel Nozzle-The Determining Interface Between Injection System and Combustion Chamber. THIESEL 2000, Valencia 13-15 September 2000.
11. C.H. Bae and J. Kang. Diesel Spray Characteristics of Common-Rail VCO Nozzle Injector. THIESEL 2000, Valencia 13-15 September 2000.
12. C. Arcoumanis and J. Whitelaw. Is Cavitation Important in Diesel Engine Injectors? THIESEL 2000, Valencia 13-15 September 2000.
13. C. Soteriou, R. Andrews and M. Smith. Diesel Injection – Laser Light Sheet Illumination of the Development of Cavitation in Orifices. Combustion Engines and Hybrid Vehicles, London, 28-30 April 1998, I.Mech.E., Paper C529/018/98
14. C. Soteriou and R. Andrews. Cavitation Hydraulic Flip and the Atomization in Direct Injection Diesel Sprays. IMechE C465/051/93
15. H. Hiroyasu and M. Arai. Structures of Fuel Sprays in Diesel Engines. SAE900475
16. J.C. Dent. A Basic Comparisons of Various Experimental Methods for Studying Spray Penetration. SAE710571
17. J. Arregle, V. Pastor and S. Ruiz. The Influence of Injection Parameters on Diesel Spray Characterization. SAE1999-01-0200
18. C. Badock, R. Wirth and C. Tropea. The influence of Hydro Grinding on Cavitation Inside a Diesel Injection Nozzle and Primary Break-up under Unsteady Pressure Conditions. Proc. 15th ILASS-Europe '99. Toulouse July 1999.
19. A.J. Yule and D.G. Salters. On the Distance Required to Atomize Diesel Sprays Injected From Orifice-Type Nozzles. Journal of Automobile Engineering, Proc IMechE Vol 209
20. R.E. Morgan, D. Kennaird, M.R. Heikal and F. Bar. Characterization of a High Pressure Diesel Fuel Spray at Elevated Pressures. THIESEL 2000, Valencia 13-15 September 2000.
21. D.A. Kennaird, C. Crua, M.R. Heikal, R.E. Morgan, F. Bar and S.M. Sapsford. A New High Pressure Diesel Spray Research Facility. International Conference on Computational and Experimental Methods in Reciprocating Engines, 1-2 November 2000.C587/040/2000
22. U. Flaid, W. Polach and G. Ziegler. Common Rail Systems (CR-Systems) for Passenger Car DI Diesel Engines; Experiences with Applications for Series Production Projects. SAE1999-01-0191.
23. A.J. Yule, D.G. Salters. On the Distance Required to Atomize Diesel Sprays Injected From Orifice-Type Nozzles. Journal of Automobile Engineering, Proc. Instn. Mech. Engrs. Vol. 209.
24. M. Mouquallid, D. Lisiecki, M. Ledoux, A. Belghit. Study of High Pressure Diesel Sprays. 14th ILASS-Europe 1998
25. B. Jawad, E. Gulari and N.A. Henein. Characteristics of Intermittent Fuel Sprays. Combustion and Flame 1992.
26. C. Heimgärtner and A. Leipertz. Investigation of the Primary Spray Breakup Close to the Nozzle of a Common – Rail High Pressure Diesel Injection System. SAE 2000-01-1799
27. K.R. Browne, I.M. Partridge, and G. Greeves. Fuel property Effects on Fuel/Air Mixing in an Experimental Diesel Engine. SAE 860223.

DEFINITIONS

Ca	Cavitation number
$\mathbf{P_a}$	Atmospheric pressure
$\mathbf{P_f}$	Fuel injection pressure
$\mathbf{P_v}$	Fuel vapour pressure
S	Fuel spray penetration
$\Delta\mathbf{P}$	Pressure difference across nozzle
ρ_a	Air density
θ	Fuel spray cone angle